SIAM J. APPL. MATH.
Vol. 70, No. 3, pp. 866–884

THERMAL-DIFFUSIVE INSTABILITY OF PREMIXED FLAMES FOR A SIMPLE CHAIN-BRANCHING CHEMISTRY MODEL WITH FINITE ACTIVATION ENERGY*

GARY J. SHARPE†

Abstract. A linear stability of freely propagating, adiabatic premixed flames is investigated in the context of a thermal-diffusive or constant density model, together with a simple two-step chain-branching model of the chemistry. This study considers the case of realistic, finite activation energy of the chain-branching step, and emphasis is on comparing with previous high activation energy asymptotic results. It is found that for realistic activation energies, a pulsating instability is absent in regimes predicted to be unstable by the asymptotic analysis. For the cellular instability, however, the finite activation energy results are in qualitative agreement with the asymptotic results, in that the flame is unstable only below a critical Lewis number of the fuel and becomes more unstable as the Lewis number is decreased. However, it is shown that very high activation energies would be required for the asymptotic analysis to be quantitatively predictive. The flame is less unstable for finite activation energies than predicted by the asymptotic analysis, in that a lower fuel Lewis number is required for instability. It is also shown that the flame structure and stability can have nonmonotonic dependencies on the activation energy.

Key words. flames, linear stability, chain-branching chemistry

AMS subject classifications. 80A25, 80A32, 75D33

DOI. 10.1137/090750366

1. Introduction.

A premixed flame is a subsonic combustion wave which propagates via diffusion of chemical species and conduction of heat between the hot burnt chemical products and the cold unburnt fuel. While, in theory, unconfined premixed flames can propagate steadily as planar waves, this may not be realized in practice due to cellular and pulsating instabilities induced by thermal-diffusive and/or hydrodynamic effects [1]. A linear stability analysis of the underlying planar wave is a first step towards understanding the origins of such instabilities and predicting the conditions under which they occur.

The majority of flame stability developments have employed a standard one-step chemistry combustion model, with a single, exothermic reaction step F→P, where F denotes fuel and P products, together with an Arrhenius form of the reaction rate. In this context, Sivashinsky [2] used a constant density model (CDM) and employed a high activation energy asymptotic (HAEA) limit in order to investigate the linear stability of one-step chemistry flames. The CDM ignores hydrodynamic effects but has extensively been demonstrated to correctly capture thermal-diffusive effects on flame dynamics [3]. Sivashinsky [2] showed that below a critical Lewis number, Le (the ratio of temperature conductivity to molecular diffusivity), the flame is unstable to a cellular instability. This cellular mode corresponds to a positive real linear eigenvalue in the stability problem. This critical value of Le is less than one, but tends to unity from below as the activation energy of the reaction is increased. Sivashinsky further showed that, above a second critical Lewis number, the flame is unstable to a

*Received by the editors February 20, 2009; accepted for publication (in revised form) May 19, 2009; published electronically July 31, 2009. The author was supported by an EPSRC Advanced Fellowship and also via Research Sponsorship from Rio Tinto Technology and Innovation.
http://www.siam.org/journals/siap/70-3/75036.html
†School of Mechanical Engineering, University of Leeds, Leeds, LS2 9JT, United Kingdom (mengjs@leeds.ac.uk).

pulsating instability corresponding to a complex conjugate pair of linear eigenvalues. The critical value of Le for pulsating instability is greater than one but again tends to unity as the activation energy is increased.

Jackson and Kapila [4] then considered the variable density model, which includes hydrodynamic effects due to thermal expansion as well as the thermal-diffusive effects, again using the one-step model in the HAEA limit. They showed that the results followed the trends predicted by the CDM study in [2]. The only qualitative difference is that there is no critical Lewis number for instability of the cellular mode. Instead the flame remains unstable to a long-wavelength hydrodynamic (Landau–Darrieus) instability above the critical Lewis number for purely thermal-diffusive instability. However, they found that the pulsating mode stability boundary was hardly affected by hydrodynamic effects.

One-step linear stability studies which do not invoke the HAEA limit, but instead employ finite (realistic) activation energies, have also been performed, both for the constant density [5] and variable density models [6, 7]. The purpose of such finite activation energy studies is twofold. First, one wishes to determine whether the high activation energy asymptotic solutions are even qualitatively predictive of the results for realistic activation energy. This is not necessarily the case for combustion problems [8, 9]. Second, these studies may provide quantitative test problems for numerical schemes designed to simulate the nonlinear regime. These simulations tend to employ moderate activation energies in order to resolve the reaction zone of the flame, in which case the HAEA results may not be quantitatively predictive of thermal-diffusive driven instabilities [5, 7]. Lasseigne, Jackson, and Jameson [5] and Sharpe and Falle [10] have demonstrated the use of the exact finite activation energy linear stability predictions for quantitative validation of numerical schemes and, moreover, used them to resolve discrepancies between results obtained by different numerical methods.

Although the one-step model has been very successful in describing and predicting many aspects of flame dynamics [1, 3], it fails to capture some qualitative features of hydrocarbon and hydrogen flame structures [1, 11]. In these fuels there any many intermediate steps in the conversion of fuel into products. These include chain-branching reactions, which produce a net increase in intermediate species such as radicals. The chain-branching reactions tend to have high activation energy, and hence are active in the high-temperature regions of the flame, where they convert the fuel into intermediate species [11]. The intermediate molecules produced may then diffuse forwards and backwards over the entire flame structure, so that the thermal conduction zone is also chemically active [1, 11]. Completion reactions, which remove the intermediates and convert them into products, tend to be temperature insensitive but highly exothermic, so that heat release occurs throughout the flame [1], in contrast to occurring only in a narrow region at the downstream end of the flame structure in the one-step model. Indeed, the exothermic completion reactions continue even after the fuel has been completely converted into intermediates, so that the fuel is exhausted interior to the flame [11], whereas in the one-step model structure the complete fuel exhaustion and final adiabatic flame temperature are reached simultaneously.

This discrepancy between the one-step model and real flame structures motivates the need for a chemistry model which better mimics the effects of chain-branching outlined above, in particular to determine whether and how the presence of intermediate species affects flame dynamics. However, for purposes of mathematical theory and modeling of flames, any improved model should still be sufficiently simple and

generic that transparent, fundamental insights can be obtained and some analytical or asymptotic progress is still possible. In this spirit, Dold and coworkers [11, 12, 13] have suggested a two-step chemistry model, consisting of a single chain-branching step, F+Y→2Y, and a single completion reaction step, Y+M→P+M. Here Y represents a lumped or "pooled" amalgam of intermediate species, and M is any species required to trigger the completion reactions but unchanged in the process. In the simplest version of this model, the branching reaction is assumed to have a high activation temperature but is thermally neutral, while the completion reaction is assumed to be temperature insensitive but releases all the heat. See [11] for a very detailed discussion which puts the two-step model and its assumptions into the context of hydrogen and hydrocarbon oxidation, including how the model parameters can be fitted to hydrogen and hydrocarbon flame structures predicted from detailed chemistry calculations.

Fundamental to the two-step model described above is the concept of a chain-branching crossover temperature, T_c, which, in regards to flame structure, is the temperature at which the rate of chain-branching balances the rate of removal of intermediates by diffusion [11]. Around this temperature a chain-branching explosion occurs in which the remaining fuel is converted rapidly into intermediates. For large activation energies of the branching step, the reaction is then active only in a narrow region occurring at temperatures close to T_c. As well as being able to mimic the main features of real flames, which the one-step model cannot, the two-step model has mathematical advantages over the one-step model. First, the simple chain-branching model does not suffer from the well-known "cold-boundary difficulty" for finite activation energies inherent in the one-step model [14]. Second, in the HAEA limit, the jump conditions across the reaction sheet are linear in the variables [11], as compared to the more complex jump conditions of the one-step model, which are nonlinear in the temperature at which the reaction sheet occurs [3]. Further, in this asymptotic limit, while the one-step model also requires a near-equidiffusional flame (NEF) approximation (Lewis number asymptotically close to unity), the two-step analysis is valid for arbitrary values of the Lewis number [11].

Dold [11] studied the linear stability of premixed flames modeled with the two-step chemistry scheme, in the context of the constant density thermal-diffusive model and employing a HAEA limit of the chain-branching reaction. He found that, as for the one-step model, the flame is predicted to be unstable to a cellular instability below a critical Lewis number of the fuel (which is less than unity) and may be unstable to the pulsating instability above another critical fuel Lewis number (greater than unity). However, unlike for the one-step model, the critical values are to leading order independent of the activation energy. Instead, the main stability parameter is the crossover temperature, T_c, which has no analogy in the one-step model. The pulsating instability disappears entirely below a threshold value of T_c, again with no analogue in the one-step model. For adiabatic flames, the wave becomes more unstable (the critical Lewis numbers for the cellular and pulsating instability both tend to unity) as T_c tends to the adiabatic temperature in the fully burnt state, T_{ad}. However, in the limit $T_c \to T_{\mathrm{ad}}$, where intermediates play a minor role in the flame structure, the two-step model stability can actually be described to leading order by the one-step model [11]. Interestingly, however, the effective activation energy of the required one-step model description is not linked to the activation energy of the chain-branching reaction, but is inversely proportional to $T_{\mathrm{ad}} - T_c$.

Sharpe [15] then extended the two-step HAEA results by considering the variable density model, hence taking into account hydrodynamics effects. As for the one-step

model, he found that the only qualitative difference from the CDM results is that the flame remains unstable to a long-wavelength hydrodynamic instability, even for Lewis numbers of the fuel above the critical value for purely thermal-diffusive induced instability. Gubernov and coworkers [16, 17, 18] then examined the linear stability of the two-step model for finite activation energies (i.e., without invoking the HAEA approximation) in the context of the CDM. They considered only one-dimensional perturbations corresponding to a purely longitudinal pulsating instability.

Hence the logical next step in the development of the two-step theory is to consider the multidimensional linear thermal-diffusive CDM stability for finite activation energies. This is the motivation for this paper, which should hence be viewed as the two-step analogue of the one-step CDM study in [5]. The purpose of the paper is twofold: first, to determine how well the HAEA analysis of [11] predicts the results of realistic, finite activation energy studies and to determine whether the HAEA results are even qualitatively correct for this problem; second, to provide a quantitative test of numerical methods for simulating the full nonlinear solutions of the two-step CDM, such as studies currently underway (L. Kagan, J. Dold, private communications). The paper is arranged as follows: the two-step CDM is described in section 2; the steady, planar flame solutions are considered in section 3; the linear stability analysis is performed in section 4, and the results given in section 5; and section 6 contains the conclusions.

2. The model. The governing equations are those of the CDM incorporating the two-step chain-branching kinetics mechanism. In two dimensions, with the flow in the x-direction, the nondimensional form of these equations is

$$\frac{\partial T}{\partial t}+\frac{\partial T}{\partial x}=\frac{\partial^2 T}{\partial x^2}+\frac{\partial^2 T}{\partial y^2}+QW_C, \tag{2.1a}$$

$$\frac{\partial F}{\partial t}+\frac{\partial F}{\partial x}=\frac{1}{Le_F}\left(\frac{\partial^2 F}{\partial x^2}+\frac{\partial^2 F}{\partial y^2}\right)-W_B, \tag{2.1b}$$

$$\frac{\partial Y}{\partial t}+\frac{\partial Y}{\partial x}=\frac{1}{Le_Y}\left(\frac{\partial^2 Y}{\partial x^2}+\frac{\partial^2 Y}{\partial y^2}\right)+W_B-W_C, \tag{2.1c}$$

where T is the temperature, F and Y are mass fractions of fuel and intermediates, respectively, Le_F and Le_Y are the Lewis numbers (ratio of temperature conductivity to molecular diffusivity) of the fuel and intermediates, Q is the dimensionless heat of reaction, and W_B and W_C are the chain-branching and completion reaction rates. These equations have solutions for which the flame is one-dimensional and steady (see section 3). Equations (2.1) are written in the rest-frame of the steady flame and have been nondimensionalized as follows:

$$\rho=\frac{\bar\rho}{\bar\rho_f},\quad u=\frac{\bar u}{\bar V_f},\quad T=\frac{\bar T}{\bar T_f}, \tag{2.2a}$$

$$x=\frac{\bar\rho_f\bar V_f\bar c_p}{\bar\kappa}\bar x,\quad y=\frac{\bar\rho_f\bar V_f\bar c_p}{\bar\kappa}\bar y,\quad t=\frac{\bar\rho_f\bar V_f^2\bar c_p}{\bar\kappa}\bar t, \tag{2.2b}$$

where a bar ($^-$) denotes dimensional quantities and an "f" subscript denotes quantities in the fresh, unburnt gas upstream of the flame. Here $\bar V_f$ is the speed of the steady, planar flame in the laboratory frame or the flow speed in the steady flame's rest-frame; $\bar c_p$ is the specific heat at constant pressure; $\bar\kappa$ is the coefficient of thermal

conductivity; and the characteristic length-scale is the heat conduction scale (usually called the "flame length"). Note from (2.2) that the nondimensional flow speed and density are unity, as is the dimensionless temperature in the fresh gas ahead of the flame.

The dimensionless chain-branching and completion reactions of the two-step model can be written in the form

$$W_B = \Lambda F Y \exp\left(\theta\left[\frac{1}{T_b} - \frac{1}{T}\right]\right), \tag{2.3a}$$

$$W_C = \Lambda Y. \tag{2.3b}$$

As usual [11, 15], we assume that the completion rate is state independent (zero activation energy), and we also assume that the chain-branching step is thermally neutral, so that all the heat, Q, is released in the completion step. Here Λ is the dimensionless completion rate constant and θ is the dimensionless activation energy of the chain-branching step. The chain-branching rate multiplier has been written in terms of a homogeneous crossover temperature, T_b. This is the temperature at which the chain-branching and completion rate multipliers are equal. For high activation energy, this marks the temperature in a homogeneous (constant volume) mixture at which a chain-branching explosion occurs, during which the fuel is very rapidly consumed. However, Dold [11] shows that an "inhomogeneous" crossover temperature, T_c, is more appropriate for flames. This is the temperature at which the chain-branching rate is equal to the rate of removal of radicals by diffusion, and hence where the chain-branching explosion occurs in a flame when the activation energy is sufficiently high. The relation between T_b and T_c [11] is given by

$$T_b = \left(\frac{1}{T_c} + \frac{2}{\theta}\ln(\theta/T_c)\right)^{-1}. \tag{2.4}$$

Hence note that T_b and T_c are equal in the HAEA limit, $\theta \to \infty$, to leading order. The Zel'dovich number (an alternative, widely used dimensionless activation energy), β, based on T_c, is defined as

$$\beta = \frac{\theta(T_c - 1)}{T_c^2}.$$

Note that Dold [11] used alternative scalings for the nondimensionalization. However, his nondimensional quantities (denoted by a "D" subscript) are simply related to those used here by

$$T_D = \frac{T}{T_c}, \quad F_D = F, \quad Y_D = \frac{Le_F}{Le_Y}Y, \quad x_D = \sqrt{Le_Y \Lambda}\,x, \quad t_D = Le_Y \Lambda t, \tag{2.5a}$$

$$Q_D = \frac{Q}{T_c - 1}. \tag{2.5b}$$

Note that in the HAEA limit, the CDM flame structure and stability depend on Q and T_c only through the combination Q_D [11]. Gubernov and coworkers [16, 17, 18, 19] use another choice of scalings. The relationships between their dimensionless space and time scales (denoted by a "G" subscript) and those used here are

$$x_G = \sqrt{\frac{Q\Lambda \exp(\theta/T_b)}{\theta}}\,x, \qquad t_G = \frac{Q\exp(\theta/T_b)}{\theta}t.$$

They also define dimensionless parameters β_G and r_G, which in terms of our scalings are

$$\beta_G = \frac{\theta}{Q}, \quad r_G = \exp\left(\frac{-\theta}{T_b}\right). \tag{2.6}$$

Their nondimensional temperature is then $u_G = T/\theta$. However, note that a somewhat different model from the one used here is considered in [16, 17, 18, 19], in that they neglect the initial temperature such that $u_G = T/\theta = 0$ in the fresh state. Hence the Arrhenius term $\exp(-1/u_G)$ is also initially zero rather than small but positive. Thus there is not a direct correspondence between their model and the one considered here and in [11].

Realistic Zel'dovich numbers for normal gaseous flames are β between about 4 and 6 for hydrogen and hydrocarbon oxidation [11], corresponding to a value of $\theta \approx 30$ for an initial temperature of 300 K. The representative range of heats of reaction for these fuels is $4 < Q < 9$ [20]. Here we set $Q = 5$ unless otherwise specified. Appropriate values of Lewis numbers are between 0.3 and 1.8, with the lower bound corresponding to lean hydrogen [11] and the upper bound to propane [21]. However, since the flame stability is found to be not very sensitive to the Lewis number of the intermediates [11, 15], in this paper Le_Y is set to unity throughout, and we concentrate on the effect of varying Le_F.

3. Steady, planar flames. For finite activation energies, the underlying steady one-dimensional flame solution needs to be determined numerically. Planar flame solutions of the two-step CDM have been numerically investigated previously in [16, 17, 18, 19], albeit for a different form of the model in which the upstream temperature is neglected. However, these studies mainly examined the effect of changing the activation energy through changes in the quantity β_G but with r_G held constant, which has the effect of varying θ and T_c simultaneously in such a way that the results are limited to a low activation energy regime. Here, however, we are interested in the effect of varying activation energy for fixed crossover temperature, including investigating the convergence to the HAEA results and comparing and contrasting the HAEA solutions with those for realistic values of θ. Furthermore, we also need to develop the asymptotic forms of the steady solution as $x \to \pm\infty$ for the purposes of the linear stability method employed in section 4.

For steady, planar flames the governing equations (2.1) can be reduced to the system

$$\frac{dT_0}{dx} = T_0 - 1 + Q(X_0 + Z_0 - 1), \tag{3.1a}$$

$$\frac{dF_0}{dx} = Le_F(F_0 - X_0), \tag{3.1b}$$

$$\frac{dY_0}{dx} = Le_Y(Y_0 - Z_0), \tag{3.1c}$$

$$\frac{dX_0}{dx} = -W_B, \tag{3.1d}$$

$$\frac{dZ_0}{dx} = W_B - W_C, \tag{3.1e}$$

where a zero subscript denotes quantities in the steady, planar flame solution and where the variables X_0 and Z_0 are defined by (3.1b,c). The initial, fresh state corresponds to $x \to -\infty$; i.e., the flame propagates from right to left in the laboratory frame. Hence $dq_0/dx \to 0$ (where q_0 denotes any dependent variable) and $T_0 = F_0 = 1$, $Y_0 = 0$ as $x \to -\infty$. Since $F_0 = 1$ and $dF_0/dx = 0$ in this limit, we must have $X_0 = 1$ as $x \to -\infty$, by (3.1b). Similarly, $Z_0 = 0$ in this limit, by (3.1c).

The burnt state corresponds to $x \to \infty$. For finite activation energies, some residual fuel can be left after the chain-branching reaction is complete and the intermediates have been consumed [12, 18]. Hence the appropriate boundary conditions as $x \to \infty$ are $dq_0/dx \to 0$, $F_0 = F_\infty$, $T_0 = T_\infty = 1 + Q(1 - F_\infty)$, $Y_0 = 0$, where F_∞ is the fuel mass fraction left over in the burnt state, to be determined. Equations (3.1b) and (3.1c) then give $X_0 = F_\infty$ and $Z_0 = 0$, respectively, as $x \to \infty$. For other parameters fixed, both sets of boundary conditions can be simultaneously satisfied only for a certain value of Λ. Note that Λ is a ratio of a Damköhler number to the square of the flame's Mach number [7], where the Damköhler number is a ratio of diffusion to reaction times. Hence for a fixed Damköhler number, Λ plays the role of the flame speed eigenvalue.

We will solve the eigenvalue problem by numerical shooting. For this purpose, and for the linear stability analysis, the asymptotic solutions valid for large $|x|$ are required. As $x \to -\infty$, by considering the linearization about the fresh state, the asymptotic solution to equations (3.1) can be shown to be

$$T_0 \sim 1 + \beta_T Y_0^{1/h_1} - \frac{Q\Lambda}{h_1(h_1 - 1)} Y_0, \tag{3.2a}$$

$$F_0 \sim 1 + \beta_F Y_0^{Le_F/h_1} - \frac{Le_F \Lambda e_f}{h_1(h_1 - Le_F)} Y_0, \quad e_f = \exp\left[\theta\left(\frac{1}{T_b} - 1\right)\right], \tag{3.2b}$$

$$X_0 \sim 1 - \frac{\Lambda e_f}{h_1} Y_0, \quad Z_0 \sim \frac{\Lambda(e_f - 1)}{h_1} Y_0, \tag{3.2c}$$

$$Y_0 \sim \alpha_1 \exp(h_1 x), \quad h_1 = \frac{1}{2}\left(Le_Y + \sqrt{Le_Y^2 + 4Le_Y \Lambda(1 - e_f)}\right), \tag{3.2d}$$

where β_T, β_F, and α_1 are constants of integration, to be determined.

As $x \to \infty$, the linearization about the burnt state gives the asymptotic solution to be

$$T_0 \sim 1 + T_\infty - \frac{Q\Lambda e_b}{h_2(h_2 - 1)} Y_0, \quad e_b = F_\infty \exp\left[\theta\left(\frac{1}{T_b} - \frac{1}{T_\infty}\right)\right], \tag{3.3a}$$

$$F_0 \sim F_\infty + \frac{Le_F \Lambda e_b}{h_2(h_2 - Le_F)} Y_0, \tag{3.3b}$$

$$X_0 \sim F_\infty - \frac{\Lambda e_b}{h_2} Y_0, \quad Z_0 \sim \frac{\Lambda(e_b - 1)}{h_2} Y_0, \tag{3.3c}$$

$$Y_0 \sim \alpha_2 \exp(h_2 x), \quad h_2 = \frac{1}{2}\left(Le_Y - \sqrt{Le_Y^2 + 4Le_Y \Lambda(1 - e_b)}\right), \tag{3.3d}$$

where α_2 is a constant of integration.

For sufficiently small Y_0, (3.2) and (3.3) can be used as initial conditions for numerical integrations of (3.1) from either the fresh or burnt states, respectively.

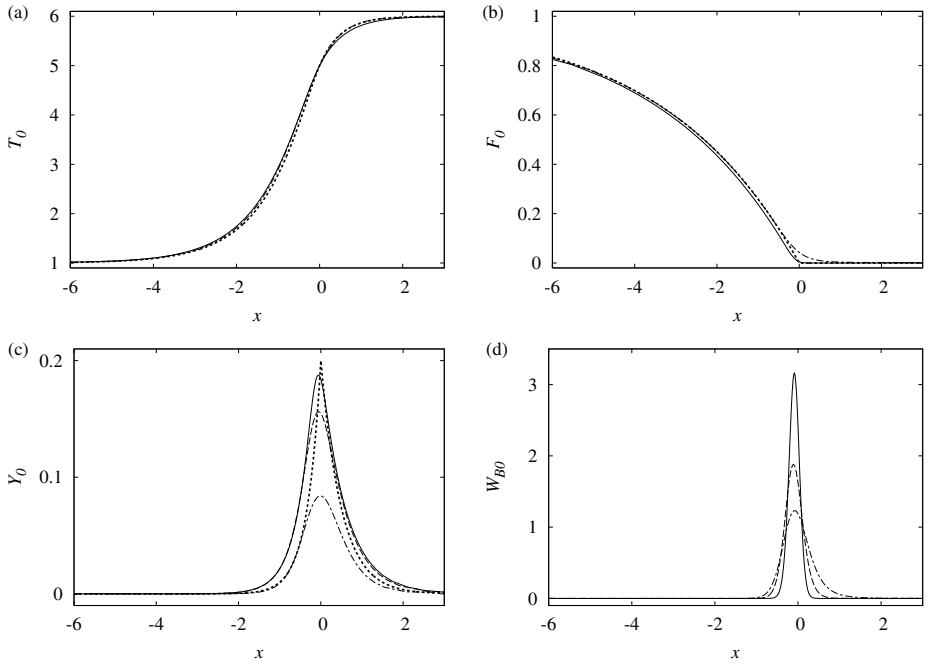

FIG. 3.1. *Spatial profiles of* (a) *temperature,* (b) *and* (c) *fuel and intermediate fractions, and* (d) *chain-branching reaction rate in the steady solution for* $Q = 5$, $T_c = 5$, $Le_F = 0.3$, $Le_Y = 1$, *and* $\theta = 120$ *(solid lines),* 60 *(dashed lines), and* 30 *(dot-dashed lines), corresponding to Zel'dovich numbers of* $\beta = 19.2$, 9.6, *and* 4.8, *respectively. (Note* $\theta = 60$ *not shown in* (a) *or* (b) *for clarity.) Also shown is the HAEA solution (dotted lines).*

Since equations (3.1) are autonomous and since temperature is monotonic and spans a finite domain, T_0 is used as the independent variable in the integrations. Note also that the spatial origin is arbitrary. Here we choose $x = 0$ to correspond to the point where $T_0 = T_c$. The solutions from both boundaries are integrated to a midpoint where $T_0 = 1 + Q/2$. In the required solution, the values of F_0, Y_0, X_0, and Z_0 obtained by starting the integration from either boundary must match at this point. This matching is achieved by Newton–Raphson iterations on the values of Λ, β_T, β_F, and F_∞.

Figure 3.1 shows the steady, planar flame structure when $Q = T_c = 5$ for a low Lewis number of $Le_F = 0.3$ (relevant to cellular instability regimes) and for various activation energies ($\theta = 30$, 60, and 120, corresponding to Zel'dovich numbers $\beta = 4.8$, 9.7, and 19.2, respectively). For comparison, the HAEA solution is also shown. In the HAEA limit, for temperatures much below T_c the chain-branching reaction rate is exponentially small, and hence there is essentially no branching in the region of the flame corresponding to temperatures below this. For temperatures much above T_c, however, the rate is then exponentially large and must be limited by the extremely rapid complete conversion of the fuel into intermediates. Thus to leading order, the reaction rate (2.3a) can be replaced by a chain-branching reaction "sheet" or surface on which the fuel is depleted and converted into intermediates, and across which jump conditions can be applied. In particular, the profiles in F_0 (and Y_0) have jump discontinuities in the gradient at $T = T_c$ in this asymptotic limit [11].

The spatial temperature profiles in Figure 3.1(a) are quite similar to each other

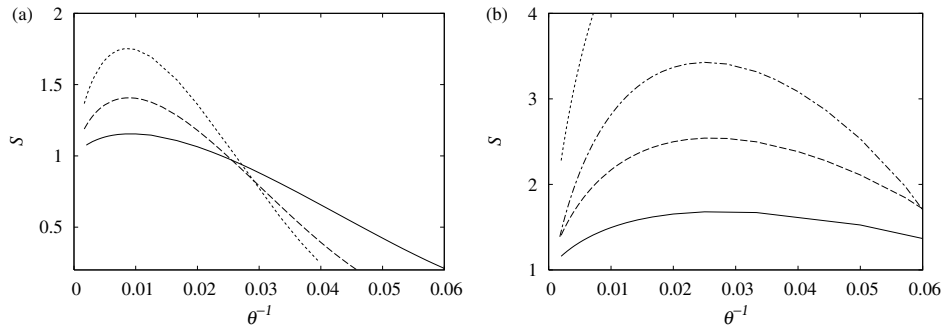

FIG. 3.2. *Flame speed relative to HAEA value as a function of inverse activation energy for* $Q = 5$, $Le_Y = 1$ *and* (a) $Le_F = 0.3$ *and* $T_c = 5$ *(solid line),* 5.5 *(dashed line), and* 5.7 *(dotted line);* (b) $Le_F = 1.8$ *and* $T_c = 5$ *(solid line),* 5.5 *(dashed line), and* 5.8 *(dot-dashed line). Also shown in* (b) *is the case* $Le_F = 2.6$ *and* $T_c = 5.8$ *(dotted line).*

and to the HAEA prediction. The fuel fractions in Figure 3.1 profiles are also very close, apart from when F_0 becomes small. For finite activation energies, the branching-reaction rate is appreciable over a range of temperatures around T_c; i.e., there is a chain-branching reaction zone region of finite width (Figure 3.1(d)). The lower θ, the wider the reaction zone and the smaller the maximum rate attained, due to the decreased sensitivity of the rate on temperature. Thus, instead of a gradient discontinuity, as in the HAEA limit, the gradient in F_0 changes smoothly within the reaction zone as it approaches its final value. The lower θ, the slower F_∞ is approached (Figure 3.1(b)), due to the widening reaction zone. However, the main difference between the flame structures for varying activation energy is in the intermediate profiles. Figure 3.1(c) shows that in this case, the peak value of Y_0 decreases with θ. This is again due to the slower branching reaction rate and hence increased role of competition with removal of intermediates by diffusion and completion reaction.

The flame speed relative to the HAEA value is a useful measure of the dependence of the solution on activation energy. This is given by

$$S = \sqrt{\frac{\Lambda_\infty}{\Lambda}},$$

where Λ_∞ is the value of the flame eigenvalue in the HAEA limit, determined in [11, 15]. Figure 3.2(a) shows S as a function of the inverse activation energy, θ^{-1}, for $Q = T_c = 5$ and $Le_F = 0.3$ (corresponding to the profiles shown in Figure 3.1), which reveals that the flame speed dependence on the activation energy is not monotonic: as θ^{-1} is increased from zero, the flame speed initially increases above the asymptotic value and reaches a maximum value (of $S = 1.15$ at $\theta = 110$ in this case) before decreasing for lower activation energies. Such nonmonotonic behaviors with activation energy appear to be a feature of the two-step model, including the dependence of flame-ball solutions [12] and the stability of the planar solution discussed in section 5. Note that, as θ is decreased further, more fuel begins to escape the chain-branching reaction zone, due to the slower reaction rate and hence the inability of the reaction to produce a significant build-up of intermediates before they are removed by diffusion and completion. Hence the peak amount of intermediates becomes very small at low values of θ, with significant amounts of residual fuel left over. In fact, for $Le_F \leq 1$, an activation energy extinction limit occurs, below which there is no steady solution [18].

Indeed, the flame speed drops to zero at a sufficiently small activation energy, which occurs when e_b reaches unity, where e_b is defined in (3.3a) [18]. However, for the parameter ranges studied here, this is an effect which occurs only at unrealistically low θ, and hence we do not investigate it further.

Also shown in Figure 3.2(a) are the dependencies of S on θ for values of the crossover temperature $T_c = 5.5$ and $T_c = 5.7$, still with $Q = 5$ and $Le_F = 0.3$. This shows that as $T_c \to 1 + Q$, the flame speed becomes increasingly sensitive to the activation energy, in that the flame speed initially increases more rapidly with θ^{-1}; i.e., increasingly large activation energies are required for the HAEA value to be quantitatively predictive as T_c is increased. This is due to the fact that, in the HAEA solution, the length scale of the intermediate diffusion zone, in which completion reactions and heat release occur, rapidly becomes shorter as $T_c \to 1 + Q$ [11, 15]. While in the asymptotic limit the chain-branching zone remains infinitesimally thin compared to this heat release zone, for the finite activation energy solutions θ must be sufficiently high for the width of the finite chain-branching zone to be rendered thin compared to the heat release length scales. Thus, since the heat release zone narrows rapidly as $T_c \to 1+Q$, higher values of θ are required for the chain-branching zone width to be negligible in comparison and hence for the HAEA solution to be quantitatively correct. Note from Figure 3.2(a) that for higher crossover temperatures the peak value of S as a function of θ is higher, and the flame speed also drops more rapidly subsequent to the peak value.

Figure 3.2(b) shows S as a function of the inverse activation energy for a high fuel Lewis number, $Le_F = 1.8$ (relevant to the pulsating instability), and various crossover temperatures ($T_c = 5$, 5.5, and 5.8). While in the HAEA solution the flame speed is independent of Le_F [11], Figures 3.2(a) and (b) show there is a strong dependence on the fuel Lewis number for finite activation energies. Indeed, for a given T_c, the flame speed is even more sensitive to θ^{-1} for higher fuel Lewis numbers, in that S increases faster and departs further from the asymptotic value than for the lower values. Hence extremely high activation energies are required for the HAEA analysis to be quantitatively predictive for the $Le_F = 1.8$ case. This is due to the fuel diffusion zone scale rapidly becoming narrower as Le_F is increased. Hence a larger activation energy will be required to render the chain-branching reaction zone thin compared to this diffusion length and thus for the HAEA reaction sheet assumption to be valid. The peak flame speed also occurs at smaller activation energy for $Le_F = 1.8$ than for $Le_F = 0.3$. Note that for $Le_F > 1$ and for sufficiently low activation energy the flame speed actually approaches a turning point at a nonzero value of S [18]. For activation energies below this extinction turning point, there is no solution, but there is then a second very low-speed solution branch for a range of activation energies above the extinction value [18]. However, again for the parameter sets considered here, these effects are found to occur only at unrealistically small activation energies and hence are not considered herein.

Figure 3.3 shows the steady structure for $Le_F = 1.8$ and $T_c = 5.8$, values chosen as both a sufficiently high fuel Lewis number and a crossover temperature sufficiently close to the adiabatic flame temperature are required for the pulsating instability to manifest according to the asymptotic theory [11, 15]. Figure 3.3 shows that in this case not only does the flame speed depart significantly (by over a factor of three for realistic activation energies) from the HAEA value, but the flame structure is also quite different from the asymptotic prediction. First, Figure 3.3(a) shows that the temperature in the finite activation energy cases approaches T_∞ much more slowly than in the HAEA limit. The HAEA solution in this high T_c case resembles a one-

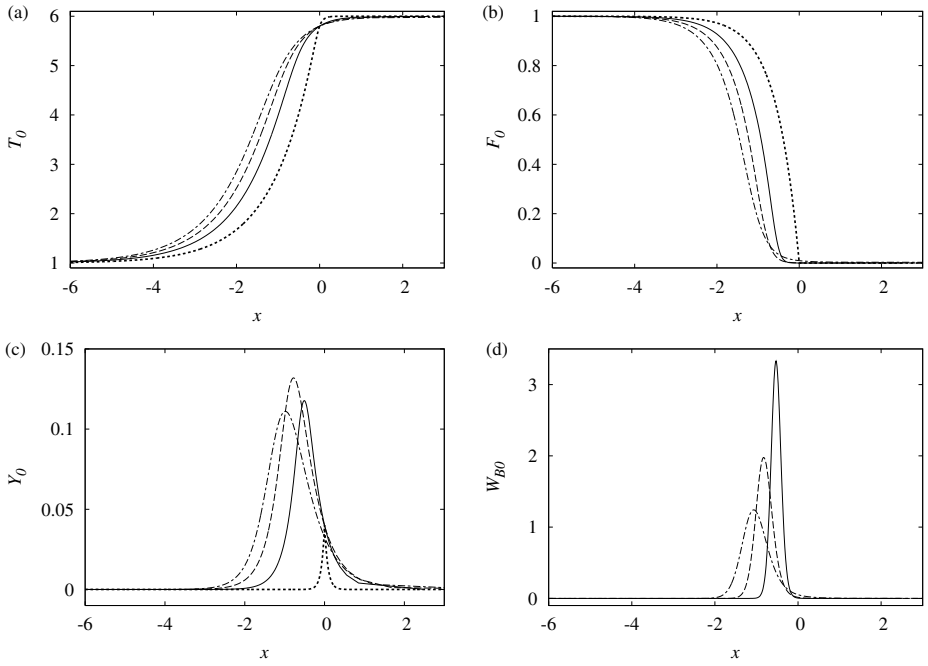

FIG. 3.3. *Spatial profiles of* (a) *temperature,* (b) *and* (c) *fuel and intermediate fractions, and* (d) *chain-branching reaction rate in the steady solutions for* $Q = 5$, $T_c = 5.8$, $Le_F = 1.8$, $Le_Y = 1$, *and* $\theta = 120$ *(solid lines),* 60 *(dashed lines), and* 30 *(dot-dashed lines), corresponding to Zel'dovich numbers of* $\beta = 19.2$, 9.6, *and* 4.8, *respectively. Also shown is the HAEA solution (dotted lines).*

step HAEA structure [11], in which there is a gradient discontinuity in T_0 at the point where the temperature reaches $1 + Q$, while for the two-step model with finite activation energy the temperature approaches the final value quite smoothly. Second, the estimate of the inhomogeneous crossover temperature T_c given by (2.4) no longer predicts well the temperature at which the chain-branching rate is maximum (Figure 3.3(d)). However, the main difference between the finite activation energy and the HAEA solutions in this case is in the intermediate profiles shown in Figure 3.3(c). In the HAEA limit, Y_0 has a very low peak value, and hence intermediates are present in small amounts only in a narrow region around $x = 0$. In the finite θ solutions, however, the chain-branching reaction zone is wider than the intermediate diffusion zone length of the HAEA prediction. The reaction sheet assumption of the asymptotic theory is thus not valid for the finite activation energies. The chain-branching reaction zone lengths in Figure 3.3(d) are also comparable to the fuel diffusion zone scales in Figure 3.3(b). The result is a significant build-up of intermediates which are diffused over a significant region of the flame, and hence intermediates have a much more important role in the structure for finite activation energies. Note also that the peak value of Y_0 has a nonmonotonic dependence on the activation energy.

4. Linear stability. We now assume a small normal modes perturbation to the steady flame such that

$$q(x, y, t) = q_0(x) + \epsilon q_1(x) \mathrm{e}^{\sigma t} \mathrm{e}^{iky}, \quad \epsilon \ll 1,$$

where q represents any of T, F, and Y; σ is the (complex) growth rate; and k is the wavenumber of the disturbance in the y-direction. If there are any values of σ having positive real part for any k, then the perturbation will grow in time, and the steady flame structure is unstable. The reaction rates are expanded in ϵ as

$$W_B = W_{B0} + \epsilon \mathrm{e}^{\sigma t}\mathrm{e}^{iky} W_{B0}\left(\frac{\theta}{T_0^2}T_1 + \frac{1}{F_0}F_1 + \frac{1}{Y_0}Y_1\right) + \cdots,$$

$$W_C = \Lambda Y_0 + \epsilon \mathrm{e}^{\sigma t}\mathrm{e}^{iky}\Lambda Y_1 + \cdots,$$

where

$$W_{B0} = \Lambda F_0 Y_0 \exp\left(\theta\left[\frac{1}{T_b} - \frac{1}{T_0}\right]\right).$$

We also define the following variables:

$$\tau_1 = \frac{dT_1}{dx}, \quad X_1 = F_1 - \frac{1}{Le_F}\frac{dF_1}{dx}, \quad Z_1 = Y_1 - \frac{1}{Le_Y}\frac{dY_1}{dx}.$$

The linearized versions of equations (2.1) can then be written in the form

$$\frac{d\mathbf{u}}{dx} = \mathbf{A}\mathbf{u}, \tag{4.1}$$

where $\mathbf{u} = (T_1, F_1, Y_1, \tau_1, X_1, Z_1)^T$ and

$$\mathbf{A} = \begin{bmatrix} 0 & 0 & 0 \\ 0 & Le_F & 0 \\ 0 & 0 & Le_Y \\ \sigma + k^2 & 0 & -Q\Lambda \\ -W_{B0}\theta/T_0^2 & -W_{B0}/F_0 - \sigma - k^2/Le_F & -W_{B0}/Y_0 \\ W_{B0}\theta/T_0^2 & W_{B0}/F_0 & W_{B0}/Y_0 - \sigma - k^2/Le_Y - \Lambda \end{bmatrix} \begin{bmatrix} 1 & 0 & 0 \\ 0 & -Le_F & 0 \\ 0 & 0 & -Le_Y \\ 1 & 0 & 0 \\ 0 & 0 & 0 \\ 0 & 0 & 0 \end{bmatrix}.$$

In order to solve the eigenvalue problem by shooting, we need to first determine the asymptotic forms of the solutions to (4.1) valid as $x \to \pm\infty$.

4.1. Asymptotic solution as $x \to -\infty$. Consider first the asymptotic solutions of (4.1) as the fresh state is approached, $x \to -\infty$, where $T_0 \to 1$, $F_0 \to 1$, and $Y_0 \to 0$. Hence, using the expansions (3.2) and changing to Y_0 as the independent variable, we can expand (4.1) as

$$h_1 Y_0 \frac{d\mathbf{u}}{dY_0} = \left(\mathbf{A}_0 + Y_0\mathbf{A}_1 + Y_0^{1/h_1}\mathbf{A}_2 + Y_0^{Le_F/h_1}\mathbf{A}_3 + \cdots\right)\mathbf{u}, \tag{4.2}$$

where the $\mathbf{A}_i$ now depend only on the parameters and σ and k, and $\mathbf{A}_0$ is the value of the matrix $\mathbf{A}$ evaluated at $Y_0 = 0$, $T_0 = F_0 = 1$. Equation (4.2) has six independent solutions of the form

$$\mathbf{u} = \tilde{\mathbf{u}}_i = Y_0^{\lambda_i}\mathbf{a}_{0i} + \cdots \quad \text{as } Y_0 \to 0, \quad i = 1, \ldots, 6,$$

where $h_1\lambda_i$ and $\mathbf{a}_{0i}$ are the eigenvalues and eigenvectors of $\mathbf{A}_0$. The eigenvalues of $\mathbf{A}_0$ are

$$\frac{1 \pm \sqrt{1+4(\sigma+k^2)}}{2}, \qquad \frac{Le_F \pm \sqrt{Le_F^2+4(\sigma Le_F+k^2)}}{2},$$
$$\frac{Le_Y \pm \sqrt{Le_Y^2+4(\sigma Le_Y+k^2+\Lambda Le_Y(1-e_f))}}{2}.$$

For $Re(\sigma) > 0$, the eigenvalues with a negative sign are unbounded as $Y_0 \to 0$ and must be discarded. We are hence left with three linearly independent, bounded asymptotic solutions, denoted by $i = 1, 2, 3$, say, as $x \to -\infty$.

4.2. Asymptotic solution as $x \to \infty$. Consider next the asymptotic solution of (4.1) as the burnt state is approached, i.e., as $x \to \infty$, where $T_0 \to T_\infty$, $F_0 \to F_\infty$, and $Y_0 \to 0$. Using the expansions (3.3), and once again changing to Y_0 as the independent variable, we can expand (4.1) as

$$h_2 Y_0 \frac{d\mathbf{u}}{dY_0} = (\mathbf{A}_0^* + Y_0\mathbf{A}_1^* + \cdots)\,\mathbf{u}, \tag{4.3}$$

where again the $\mathbf{A}_i^*$ depend only on the parameters and σ and k, and $\mathbf{A}_0^*$ is the matrix $\mathbf{A}$ evaluated at $Y_0 = 0$, $T_0 = T_\infty$, $F_0 = F_\infty$. Equation (4.3) has six independent solutions of the form

$$\mathbf{u} = \hat{\mathbf{u}}_i = Y_0^{\lambda_i^*}\mathbf{a}_{0i}^* + \cdots \quad \text{as } Y_0 \to 0, \quad i = 1, \ldots, 6,$$

where $h_2\lambda_i^*$ and $\mathbf{a}_{0i}^*$ are the eigenvalues and eigenvectors of $\mathbf{A}_0^*$. The eigenvalues of $\mathbf{A}_0^*$ are

$$\frac{1 \pm \sqrt{1+4(\sigma+k^2)}}{2}, \qquad \frac{Le_F \pm \sqrt{Le_F^2+4(\sigma Le_F+k^2)}}{2},$$
$$\frac{Le_Y \pm \sqrt{Le_Y^2+4(\sigma Le_Y+k^2+\Lambda Le_Y(1-e_b))}}{2}.$$

For $Re(\sigma) > 0$, the eigenvalues with a positive sign are unbounded as $Y_0 \to 0$ and must be discarded. We are again left with three linearly independent bounded solutions, denoted by $i = 1, 2, 3$, say, valid as $x \to \infty$.

4.3. Numerical solution of linearized equations. In summary, (4.1) is to be solved subject to the asymptotic forms of the solution as $x \to \pm\infty$ determined in sections 4.1 and 4.2. This entails a discrete eigenvalue problem for the linear growth rate σ when k and all other parameters are fixed. The procedure to determine the eigenvalue is as follows. First, each of the three linearly independent, bounded solutions valid as $x \to -\infty$, i.e., the $\tilde{\mathbf{u}}_i$, is used in turn as initial conditions with a sufficiently small Y_0 for the integration of (4.1). Again, T_0 is used as the independent variable for the purpose of the numerical integrations, and each solution is integrated up to the point where $T_0 = 1 + Q/2$. The result is hence the numerical values of the three linearly independent solutions evaluated at $T_0 = 1 + Q/2$, denoted by $\tilde{\mathbf{u}}_i^f$, say, and hence a general solution there is of the form

$$\mathbf{u}(1+Q/2) = \alpha_1\tilde{\mathbf{u}}_1^f + \alpha_2\tilde{\mathbf{u}}_2^f + \alpha_3\tilde{\mathbf{u}}_3^f, \tag{4.4}$$

where the α_i are complex constants of integration, to be determined.

Similarly, the three asymptotic solutions valid as $x \to \infty$ are used as initial conditions with a small value of Y_0 in order to integrate (4.1) from the burnt state back to $T_0 = 1+Q/2$. This results in the numerical evaluation of the three independent solutions at $T_0 = 1 + Q/2$ (denoted by $\hat{\mathbf{u}}_i^b$). The general solution there is hence

$$\mathbf{u}(1 + Q/2) = \alpha_4\hat{\mathbf{u}}_1^b + \alpha_5\hat{\mathbf{u}}_2^b + \alpha_6\hat{\mathbf{u}}_3^b, \tag{4.5}$$

where again the α_i, $i = 4, 5, 6$, are constants of integration.

Equations (4.4) and (4.5) are thus both solutions for $\mathbf{u}$ at the point where $T_0 = 1 + Q/2$, and hence they must match. This is possible only for eigenvalues of σ. Since we are interested in nontrivial solutions, for which not all the α_i are zero, we can divide through by one of them (α_6, say) so that the matching condition is

$$a_1\tilde{\mathbf{u}}_1^f + a_2\tilde{\mathbf{u}}_2^f + a_3\tilde{\mathbf{u}}_3^f = a_4\hat{\mathbf{u}}_1^b + a_5\hat{\mathbf{u}}_2^b + \hat{\mathbf{u}}_3^b,$$

where $a_i = \alpha_i/\alpha_6$. Let $a_i = b_i + \mathrm{i}c_i$, where b_i and c_i are real, and consider the quantity

$$\begin{aligned} m(\sigma) = |&(b_1 + \mathrm{i}c_1)\tilde{\mathbf{u}}_1^f + (b_2 + \mathrm{i}c_2)\tilde{\mathbf{u}}_2^f + (b_3 + \mathrm{i}c_3)\tilde{\mathbf{u}}_3^f \\ &- (b_4 + \mathrm{i}c_4)\hat{\mathbf{u}}_1^b - (b_5 + \mathrm{i}c_5)\hat{\mathbf{u}}_2^b - \hat{\mathbf{u}}_3^b|^2, \end{aligned} \tag{4.6}$$

where $|\mathbf{q}|^2 = \mathbf{q} \cdot \bar{\mathbf{q}}$. Then if σ is an eigenvalue, the b_i and c_i can be chosen such that $m = 0$. For a general value of σ we can minimize m by partially differentiating (4.6) with respect to each of the b_i and c_i and setting the results to zero, which corresponds to a minimum in m for each constant. This gives a 10×10 system of linear equations, $\mathbf{Cv} = \mathbf{r}$, where $\mathbf{v} = (b_1, c_1, \ldots, b_5, c_5)^T$ and $\mathbf{C}$ and $\mathbf{r}$ are a matrix and vector with numerically determined entries. Solving this system gives the b_i and c_i such that m is a minimum for given σ and parameters. The eigenvalues can then be determined by Newton–Raphson iteration on the condition $m(\sigma) = 0$.

5. Results.

5.1. Pulsating mode. Thorough carpet searches as well as Newton–Raphson searches in the complex σ plane were performed for $m(\sigma) = 0$ with fuel Lewis numbers greater than unity. No pulsating mode eigenvalue was found for reasonable, realistic ranges of activation energy and other parameters, including fuel Lewis numbers at the high end of the range for gases, $Le_F \approx 2$.

Recall that in the HAEA limit, the flame is found to be unstable to the pulsating mode only when the quantity $Q_D - 1$ is sufficiently small, where Q_D is defined by (2.5b), i.e., when T_c is sufficiently close to $1 + Q$. Above a critical value of Q_D (which is about 1.3 for $Le_Y = 1$ [11]), there is no pulsating instability regardless of the size of Le_F. For values of Q_D less than this critical value, Le_F must then still be sufficiently large for the flame to be unstable to the pulsating mode. As $Q_D \to 1$ ($T_c \to 1 + Q$) the values of Le_F required for instability also tend to unity. However, only for $Q_D - 1$ less than about 0.1 do flames with $Le_F < 2$ start to become unstable in the HAEA limit. Small values of $Q_D - 1$ result in intermediates having only a minor role in the HAEA flame structure, with only a small peak value of Y_0 (see the asymptotic result in Figure 3.3(c), for example, for which $Q_D - 1 = 0.04$). The HAEA analysis thus indicates that the pulsating instability is absent unless the presence of intermediates is small in the flame.

Returning now to finite activation energies, we have already seen in section 3 that, for realistic values, the flame structure is quantitatively different from the HAEA predictions for $Le_F > 1$, especially when T_c is close to $1 + Q$, corresponding to small

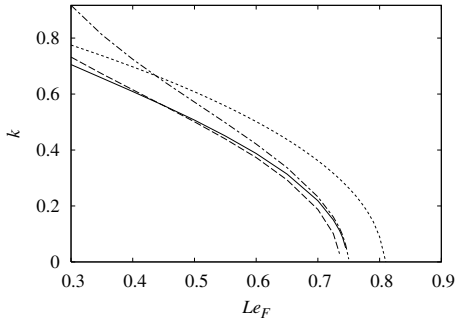

FIG. 5.1. *Neutral stability boundaries in the Le_F-k plane when $Q = 5$, $T_c = 5$, $Le_Y = 1$ for activation energies $\theta = 120$ ($\beta = 19.2$, $T_b = 3.95$) (solid line), $\theta = 60$ ($\beta = 9.6$, $T_b = 3.54$) (dashed line), and $\theta = 30$ ($\beta = 4.8$, $T_b = 3.13$) (dot-dashed line). Also shown is the boundary from the HAEA analysis (dotted line).*

$Q_D - 1$. In particular, the peak values of Y_0 are much higher than the HAEA solution predicts (Figure 3.3(c)). Furthermore, for a fixed activation energy, Figure 3.2(b) shows that as $Q_D - 1$ is decreased, the steady flame speed (and hence structure) departs further from the asymptotic prediction. The solution is also found to depart further from the HAEA prediction as Le_F is increased, for fixed θ and T_c. This is illustrated in Figure 3.2(b), which also shows S as a function of θ for $Le_F = 2.6$ when $T_c = 5.8$ and $Q = 5$ ($Q_D = 1.04$). The more significant role of intermediates in the flame structures with finite θ for high Le_F and low $Q_D - 1$ results in the stabilization of the flame. Hence even though the HAEA analysis may predict instability, the pulsating mode is absent for realistic activation energy. This absence of the pulsating instability has also been confirmed by recent direct numerical simulations of the two-step CDM equations with realistic activation energy (L. Kagan, private communication).

It should be noted that, for $Le_F > 1$, the flame does become unstable to a one-dimensional pulsating instability for sufficiently small activation energies which are very close to the extinction turning point value [18]. For such low values, the peak in the intermediates again becomes very small. However, this corresponds to a structure fundamentally different from the HAEA one. In the low θ extinction region, Y_0 remains small due to the weak temperature dependence of the chain-branching reaction and hence a rate which remains too small to significantly compete with removal of intermediates by diffusion and completion. This also results in large amounts of residual fuel escaping the branching reaction zone. Since the extinction behavior only occurs at unrealistically low activation energies for the parameter ranges considered here (and hence might be viewed as a low θ pathology of the two-step model for our cases, rather than being a realistic feature), we do not investigate this further.

5.2. Cellular instability. In the finite activation energy calculations, as predicted by the HAEA analysis, it is found that the cellular mode, for which σ is real, is always unstable, provided that Le_F is sufficiently low. The parametric dependencies on activation energy of the cellular instability boundaries, including comparisons with the HAEA predictions, are investigated below.

5.2.1. T_c fixed. Figure 5.1 shows the neutral stability boundaries (wavenumbers for which $\sigma = 0$) as a function of fuel Lewis numbers, for various activation energies in the case when the inhomogeneous crossover temperature is fixed at $T_c = 5$. The

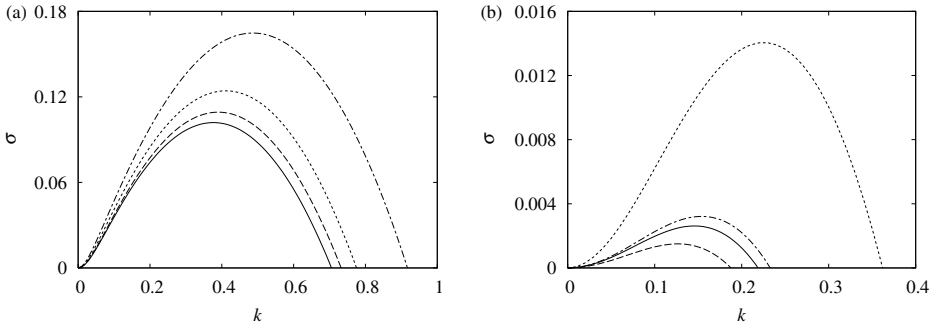

FIG. 5.2. *Growth rate versus wavenumber for* $Q = 5$, $T_c = 5$, $Le_Y = 1$, *and* (a) $Le_F = 0.3$ *and* (b) $Le_F = 0.7$ *for activation energies* $\theta = 120$ *(*$\beta = 19.2$, $T_b = 3.95$*) (solid lines),* $\theta = 60$ *(*$\beta = 9.6$, $T_b = 3.54$*) (dashed lines), and* $\theta = 30$ *(*$\beta = 4.8$, $T_b = 3.13$*) (dot-dashed lines). Also shown is the result from the HAEA analysis (dotted lines).*

flame is unstable ($\sigma > 0$) to wavenumbers in the region below the neutral stability boundaries and stable above them. Also shown for comparison is the HAEA prediction. Note first that the HAEA analysis does predict the correct qualitative trends of the finite θ results in that in every case the flame becomes unstable at a critical value of Le_F and then becomes more unstable (the range of unstable wavenumbers widens) as Le_F is further decreased. On the other hand, it is clear from Figure 5.1 that an unphysically large activation energy would be required for the HAEA solution to be quantitatively predictive of the stability boundaries. The flame is actually less unstable for finite activation energies than in the HAEA limit, in the sense that a lower fuel Lewis number is required for instability than the HAEA analysis predicts. However, note that the critical Lewis number has a nonmonotonic dependence on θ. The HAEA analysis predicts the critical value of Le_F to be 0.807, while the critical value is 0.747 for $\theta = 120$, slightly lower at 0.736 for $\theta = 60$, but higher again at 0.748 for $\theta = 30$.

Figure 5.1 also shows that the neutral stability boundaries for different activation energies can cross. Figure 5.2 shows the dispersion relations (growth rate, σ, against wavenumber of disturbance, k) for the different activation energies when $Le_F = 0.3$ and when $Le_F = 0.7$. Note that, in general, a higher value of the neutrally stable wavenumber at a fixed Le_F also corresponds to a more unstable flame in the sense that the maximum growth rate is larger (as is the wavenumber at which the maximum growth rate occurs). Thus, due to the crossing of the neutral stability curves, the most unstable value of the activation energy depends on the fuel Lewis number. In Figure 5.2(a), corresponding to $Le_F = 0.3$, $\theta = 30$ is the most unstable of the four values of activation energy shown, while $\theta = 120$ is the least unstable. However, Figure 5.2(b) shows that when Le_F is increased to 0.7, the highest growth rate is attained in the HAEA limit, while $\theta = 60$ is the least unstable case.

5.2.2. T_b fixed. Figure 5.3 shows the effect of varying the activation energy when the homogeneous crossover temperature, T_b, is kept fixed. Here $T_b = 3.54$ is used, corresponding to $T_c = 5$ when $\theta = 60$. Figure 5.3 reveals that, for fixed T_b, decreasing the activation energy has quite a strong destabilizing effect, in that the critical value of Le_F for instability increases, as does the range of unstable wavenumbers at a fixed Le_F. This is due to the dependence of T_c on θ and T_b, as given by (2.4). For the range of activation energies considered here, T_c increases as the acti-

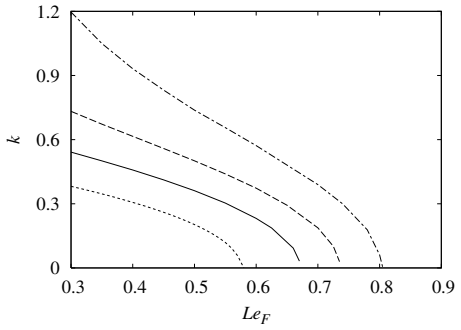

FIG. 5.3. *Neutral stability boundaries in the Le_F-k plane when $Q = 5$, $T_b = 3.54$, $Le_Y = 1$ for activation energies $\theta = 110$ ($\beta = 19.2$, $T_c = 4.45$) (solid line), $\theta = 60$ ($\beta = 9.6$, $T_c = 5$) (dashed line), and $\theta = 40$ ($\beta = 6.0$, $T_c = 5.46$) (dot-dashed line). Also shown is the boundary from the HAEA analysis (dotted line).*

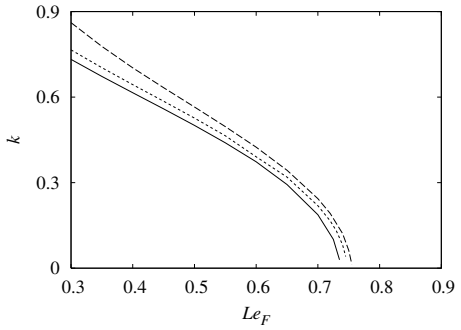

FIG. 5.4. *Neutral stability boundaries in the Le_F-k plane when $Q_D = Q/(T_c - 1) = 1.25$, $Le_Y = 1$, and $Q = 5$ with $\theta = 60$ ($T_c = 5$, $\beta = 9.6$) (solid line) $Q = 9$, $\theta = 60$ ($T_c = 8.2$, $\beta = 6.4$) (dashed line), and $Q = 9$, $\beta = 9.6$ ($\theta = 89.7$, $T_c = 8.2$) (dotted line).*

vation energy is decreased with T_b held constant: $T_c = T_b = 3.54$ in the HAEA limit, while $T_c = 4.45$, 5, and 5.46 when $\theta = 110$, 60, and 40, respectively. According to the HAEA analysis, increasing T_c towards $1 + Q$ has a major destabilizing effect on the flame [11]. Here both T_c and θ are varying, but the effect of changing T_c is much stronger than that of changing θ, so the destabilizing effect of increasing T_c dominates.

5.2.3. Q_D fixed. In the HAEA limit, the flame structure and stability depend on Q and T_c only through the combination $Q_D = Q/(T_c - 1)$. Here, we investigate whether this remains the case for finite activation energies. Figure 5.4 shows the neutral stability boundary for $Q = 5$ and $T_c = 5$ or $Q_D - 1 = 1.25$ when $\theta = 60$ ($\beta = 9.6$). Also shown are the boundaries for a larger heat of reaction $Q = 9$, but with $Q_D - 1$ held constant (so that $T_c = 8.2$) and either θ or β held fixed. This shows that increasing Q has a weak destabilizing effect for finite activation energies.

6. Conclusions. The linear stability of premixed flames has been investigated using a constant density, two-step chain-branching chemistry model in the case where the activation energy of the branching step has finite value. Emphasis was on comparing the results to the high activation energy asymptotic predictions of the model considered previously [11]. In the HAEA limit, a pulsating instability is present only if the inhomogeneous crossover temperature is sufficiently close to the adiabatic flame

temperature and then only if the Lewis number of the fuel is sufficiently high. Even then, this instability mode is suppressed for realistic activation energies and parameter regimes appropriate to gaseous flames. This is due to the much more major role of radicals in the flame than the HAEA theory predicts, leading to a more stable structure. It is possible, however, for a pulsating instability to reemerge at a low activation energy extinction limit of the two-step model [18].

The flame is found to be unstable for a cellular mode, provided that the Lewis number of the fuel is sufficiently less than unity, as predicted by the HAEA analysis. However, the HAEA results are quantitatively inaccurate in predicting the finite activation energy results. The effect of activation energy on the cellular instability is complex and depends on which quantities are fixed as the activation energy is varied. If the inhomogeneous crossover temperature, T_c, is held constant, then the critical Lewis number for instability is lower than the HAEA analysis predicts, but its value depends nonmonotonically on activation energy. The stability boundaries for different activation energies can cross each other as Le_F is varied. If the homogeneous crossover temperature is kept fixed, decreasing activation energy has a destabilizing effect due to the effective increase in T_c, so that the critical Lewis number becomes closer to unity.

In this paper we have considered adiabatic, freely propagating premixed flames. Secondary effects, such as buoyancy, heat loss, endothermic branching reaction, etc., could also be included in future linear stability studies. However, calculations of the fully nonlinear stages of the evolution, and studies of how these compare and contrast to the fully nonlinear one-step model results, would perhaps be a more important next step. Direct numerical simulations using the two-step model, along the lines of the one-step computations in Sharpe and Falle [10], will be presented in a future article. Indeed, one purpose of the present work is to provide quantitative results against which simulations can be validated.

REFERENCES

[1] C. K. Law, *Combustion Fundamentals*, Cambridge University Press, Cambridge, UK, 2006.

[2] G. I. Sivashinsky, *Diffusional-thermal theory of cellular flames*, Combust. Sci. Tech., 55 (1977), pp. 137–146.

[3] J. D. Buckmaster and G. S. S. Ludford, *Theory of Laminar Flames*, Cambridge University Press, Cambridge, UK, 1982.

[4] T. L. Jackson and A. K. Kapila, *Effect of thermal expansion on the stability of plane, freely propagating flames*, Combust. Sci. Tech., 24 (1984), pp. 191–201.

[5] D. S. Lasseigne, T. L. Jackson, and L. Jameson, *Stability of freely propagating flames revisited*, Combust. Theory Model., 3 (1999), pp. 561–611.

[6] M. A. Liberman, V. V. Bychkov, S. M. Goldberg, and D. L. Book, *Stability of a planar flame front in the slow-combustion regime*, Phys. Rev. E, 49 (1994), pp. 445–453.

[7] G. J. Sharpe, *Linear stability of planar premixed flames: Reactive Navier-Stokes equations with finite activation energy and arbitrary Lewis number*, Combust. Theory Model., 7 (2003), pp. 45–65.

[8] G. J. Sharpe and M. Short, *Ignition of thermally sensitive explosives between a contact surface and a shock*, Phys. Fluids, 19 (2007), paper 126102.

[9] A. A. Shah, R. W. Thatcher, and J. W. Dold, *Stability of a spherical flame ball in a porous medium*, Combust. Theory Model., 4 (2000), pp. 511–534.

[10] G. J. Sharpe and S. A. E. G. Falle, *Nonlinear cellular instabilities of planar premixed flames: Numerical simulations of the reactive Navier-Stokes equations*, Combust. Theory Model., 10 (2006), pp. 483–514.

[11] J. W. Dold, *Premixed flames modelled with thermally sensitive intermediate branching kinetics*, Combust. Theory Model., 11 (2007), pp. 909–948.

[12] J. W. Dold, R. W. Thatcher, A. Omon-Arancibia, and J. Redmand, *From one-step to chain-branching premixed-flame asymptotics*, Proc. Combust. Inst., 29 (2003), pp. 1519–1526.

[13] J. W. Dold, R. O. Weber, R. W. Thatcher, and A. A. Shah, *Flame balls with thermally sensitive intermediate kinetics*, Combust. Theory Model., 7 (2003), pp. 175–203.
[14] F. A. Williams, *Combustion Theory*, 2nd ed., Addison–Wesley, Jackson, MA, 1985.
[15] G. J. Sharpe, *Effect of thermal expansion on the linear stability of planar premixed flames for a simple chain-branching model: The high activation energy asymptotic limit*, Combust. Theory Model., 12 (2008), pp. 717–738.
[16] V. V. Gubernov, H. S. Sidhu, and G. N. Mercer, *Combustion waves in a model with chain branching reaction and their stability*, Combust. Theory Model., 12 (2008), pp. 407–431.
[17] V. V. Gubernov, H. S. Sidhu, G. N. Mercer, A. V. Kolobov, and A. A. Polezhaevand, *The effect of Lewis number variation on combustion waves in a model with chain-branching reaction*, J. Math. Chem., 44 (2008), pp. 816–830.
[18] V. V. Gubernov, A. V. Kolobov, A. A. Polezhaev, H. S. Sidhu, and G. N. Mercer, *Pulsating instabilities of combustion waves in a chain-branching reaction model*, Internat. J. Bifur. Chaos Appl. Sci. Engrg., 19 (2009), pp. 873–887.
[19] V. V. Gubernov, H. S. Sidhu, and G. N. Mercer, *Combustion waves in a model with chain branching reaction*, J. Math. Chem., 39 (2006), pp. 1–14.
[20] Ya. B. Zeldovich, G. I. Barenblatt, V. V. Librovich, and G. M. Makhviladze, *The Mathematical Theory of Combustion and Explosions*, Plenum Press, New York, 1985.
[21] P. Pelce and P. Clavin, *Influence of hydrodynamics and diffusion upon the stability limits of laminar premixed flames*, J. Fluid Mech., 124 (1982), pp. 219–237.